PROJECT FINAL REPORT

Grant Agreement number:	**270597**
Project acronym:	**FLOWSENSYS**
Project title:	**Efficient Flow sensor system for the separation detection at low speed in view of flight**
Funding Scheme:	**FP7-JTI-CS**
Period covered:	**from 01.02.2011 to 31.01.2014**

Name of the scientific representative of the project's co-ordinator[1], Title and Organisation:

Name:	**Wolfgang Nitsche**
Title:	**Prof. Dr.**
Organisation:	**Technische Universität Berlin**
Tel:	**+49 30 314 24449**
Fax:	**+49 30 314 22955**
E-mail:	**wolfgang.nitsche@tu-berlin.de**

[1] Usually the contact person of the coordinator as specified in Art. 8.1. of the Grant Agreement.

4.1 Final publishable summary report

Executive Summary

The VISION 2020 for European aeronautics is a “greener” aircraft and responds directly to global climate change and the ever increasing need to stay competitive in a global market. Ambitious aims are presented in this document: The 2020 aircraft is quieter and cleaner. A 50% reduction in fuel consumption per passenger kilometre would lead to 50% fewer emissions of CO2. An 80% cut in NOx emissions would significantly reduce the impact of civil air traffic on global warming and the damage to the higher atmosphere. Besides environmental aspects, another important goal for the 2020 aircraft of the European air transport system is their capability of flying safely in all weather conditions and running on schedule 99% of the time. In order to meet this vision leaps in technological developments have to be made. One of the is the improvement of the high-lift performance of airliners. One approach is the avoidance of turbulent flow separation using active flow control (AFC). An aircraft with an AFC trailing edge flap could depart and approach using steeper trajectories. Furthermore, the takeoff and landing distances could be shorter and the noise nuisance at ground could be reduced. Other aspects are enhancing maximum takeoff weight, improving safety, and reducing complexity, weight, and dimensions of flap systems and thereby lowering the direct operating cost (DOC). Those improvements would be beneficial during cruise as well and a reduction of fuel consumption is possible under certain conditions. A modern active flow control system commonly consists of three components: an actuator device that is capable of stabilizing wall-bounded flows in order to delay or suppress flow separation, an intelligent control system to realize to ensure the effective and efficient use of the energy invested, and a fluidic sensor system identify the local state of flow.

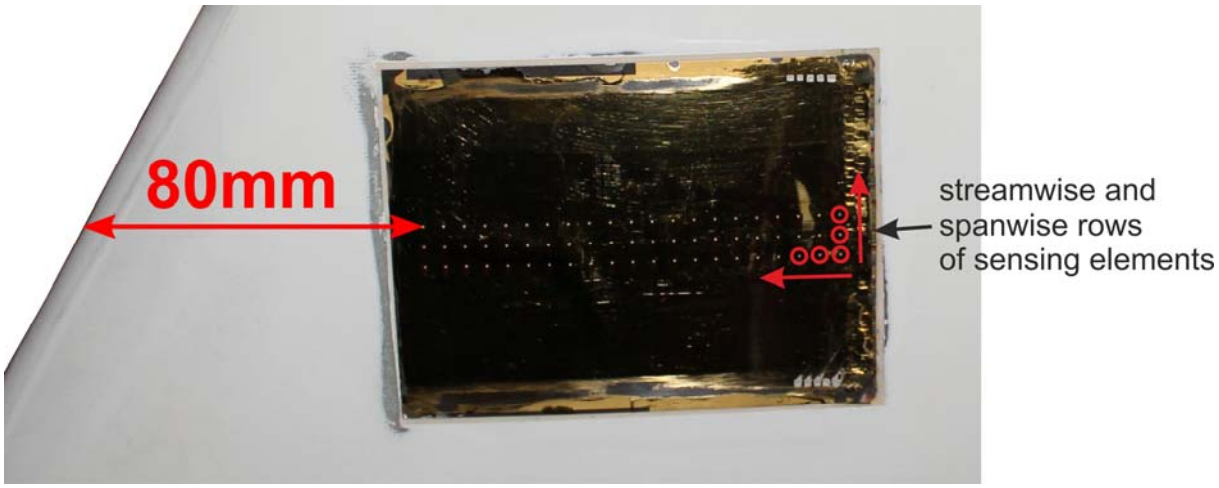

figure 1: detail view of sensor array on wing (source: EADS-IW)

The aim of FlowSenSys is to develop such an adequate sensor system, which operates in concert with an active flow control system, while providing robustness and high reliability. In the first period of this project, various sensors were tested in different flow conditions with and without separation to examine their capability of identifying the flow condition on a generic flap at moderate Reynolds and Mach numbers. The measurements were performed at the end of the first project period. In the second period the focus was on the analysis of the data recorded to evaluate the sensor performance in light of their ability to detect flow separation. Within the third and final reporting period a complex outer wing model was equipped with the most suitable sensor type and wind tunnel experiments were performed in order to validate those sensors' performance under more realistic flow conditions. It was found that the EADS micro-dot surface hot film sensors (see figure 1) are capable of detecting the state of flow by evaluating either the DC or the AC signal, which qualifies them to fulfil the requirements imposed on such a flow sensing system. Hence,

the project was successful in furthering the technology readiness level of a surface flow sensor in view of flight application.

Summary description of project context and objectives

The experimental analysis of flow separation in the boundary layer is an important aspect for the development of active flow control devices. On the one hand the highly sensitive fluidic sensors are necessary to investigate the flow phenomena during separation. On the other hand the sensors are a part of an active flow control system to allow for the adaptation of flow control parameters to the specific requirements of the flow conditions. For these applications the sensors need to be robust and sufficiently sensitive. Furthermore, when considering application on an airliner, their integration may not conflict with other design targets and maintenance procedures.

Aim of FlowSenSys was the selection and adaptation of suitable sensor concepts. Specific objectives were:

- Sensor concept development for separation detection towards application and integration in an aircraft
- Support of a system demonstration for active flow control system concept in closed loop architecture developed by SFWA partner EADS-IW; common application with an active flow control system on high-lift device.
- Wind tunnel demonstration of the sensor concept in realistic flow conditions together with SFWA partner EADS-IW

Those overall objectives translate into specific tasks. First, a review of available sensors was made to preselect those with the most promising characteristics. Parallel to that a new sensor layout was developed with special emphasis on the applicability of this concept in light of future industry application. Those sensor concept were then to be tested in generic and realistic flow conditions. Finally, a down selection of sensor concepts and designed was envisaged to be supplied to ongoing and future research projects.

Summary description of the main S&T results/foregrounds

In the first period of this project, various sensors were tested in different flow conditions with and without separation to examine their capability identifying the flow condition on a generic flap. The measurements were performed at the end of the first project period. In the second period the focus was on the analysis of the data recorded to evaluate the sensor performance in light of their ability to detect flow separation. Within the third and final reporting period a complex outer wing model was equipped with the most suitable sensor type and wind tunnel experiments were performed in order to validate those sensors' performance under more realistic flow conditions. It was found that the EADS micro-dot surface hot film sensors are capable of detecting the state of flow by evaluating either the DC or the AC signal, which qualifies them to fulfill the requirements imposed on such a flow sensing system.

First, extensive sensor test were conducted on a simple half-diffuser test section to evaluate their capability to detect flow separation. Flow visualisation experiments with tufts have been performed prior to the sensor tests to detect the position of flow separation. According to this results the flow sensors were positioned in the flow field. Three different sensor inserts were manufactured an equipped for the test. The analysis of the sensor signals and the comparison with the visualisation results showed that an effective separation detection is possible using the static pressure taps in combination with the surface mounted hot wires.

The experiments were carried out at the low speed wind tunnel at the Institute of Aeronautics and Astronautics of the Technische Universität Berlin. It is a closed circuit wind tunnel with a velocity rage from u = 3 m/s up to u = 27 m/s. All measurements were conducted on a simple half diffuser with a variable diffuser angle. A sketch of the test section is shown in Figure 2. The flow is fully turbulent due to tripping at the leading edge of the diffuser. At the End of the flat plate a turbulent boundary layer with a boundary layer thickness of $delta_{99} \approx 8$ mm has developed.

The diffuser angle of the test section can be varied from alpha = 0° to alpha = 23°. In case of alpha = 0°, the test section equals a flat plate. This configuration can be used for calibration purposes. Increasing the flap angle beyond the critical diffuser angle leads to flow separation on the flap. This separation moves upstream with increasing flap angles. Position and separation onset depend strongly on flap angel and the flow velocity.

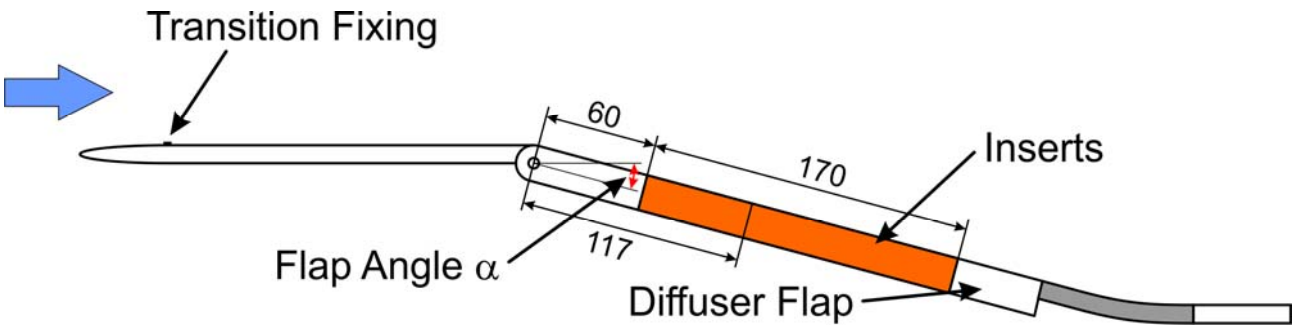

Figure 2: Sketch of the test section

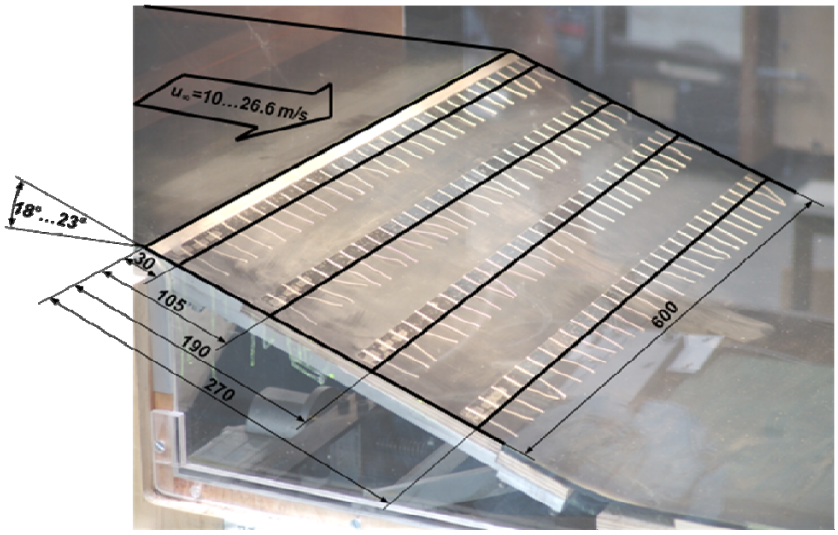

Figure 3: Experimental setup

Therefore a preliminary flow visualisation study with tufts was conducted. For this experiments the flap was equipped with four rows of tufts as can be seen Figure 3. During the experiments a digital camera was used to take pictures of the tufts on the flap. This experimental setup enables a wide variation of the flow velocity and the flap angle. According to these results the boundary conditions for the sensor test were chosen.

Figure 4 shows two images of the flap together with the extracted flow topology. For α = 19° it is apparent that the flow in the upper area is still attached to the flap, as the tufts are attached to the surface and point to the trailing edge of the flap. Due to the sidewalls of the wind tunnel a secondary flow separation develops on both sides of the flap, marked with the light blue lines. These secondary flow separation increases to the trailing edge of the flap and limits the area for the sensor test. The two-dimensional pressure-induced flow separation in the middle of the flap is marked with the red lines. As a result of the unsteady nature of flow separation it is not possible to identify a single separation line. In fact there is an area on the flap where separation occurs. Separation onset is indicated by the dashed line, and the position with a fully separated flow is marked with the solid red line.

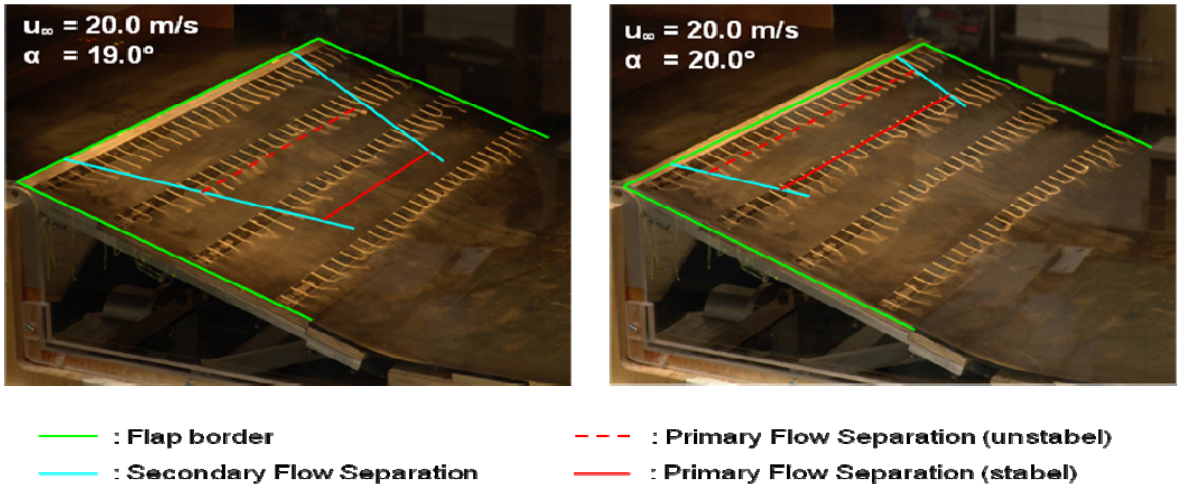

Figure 4: Tuft visualisation for u_∞ = 20 m/s

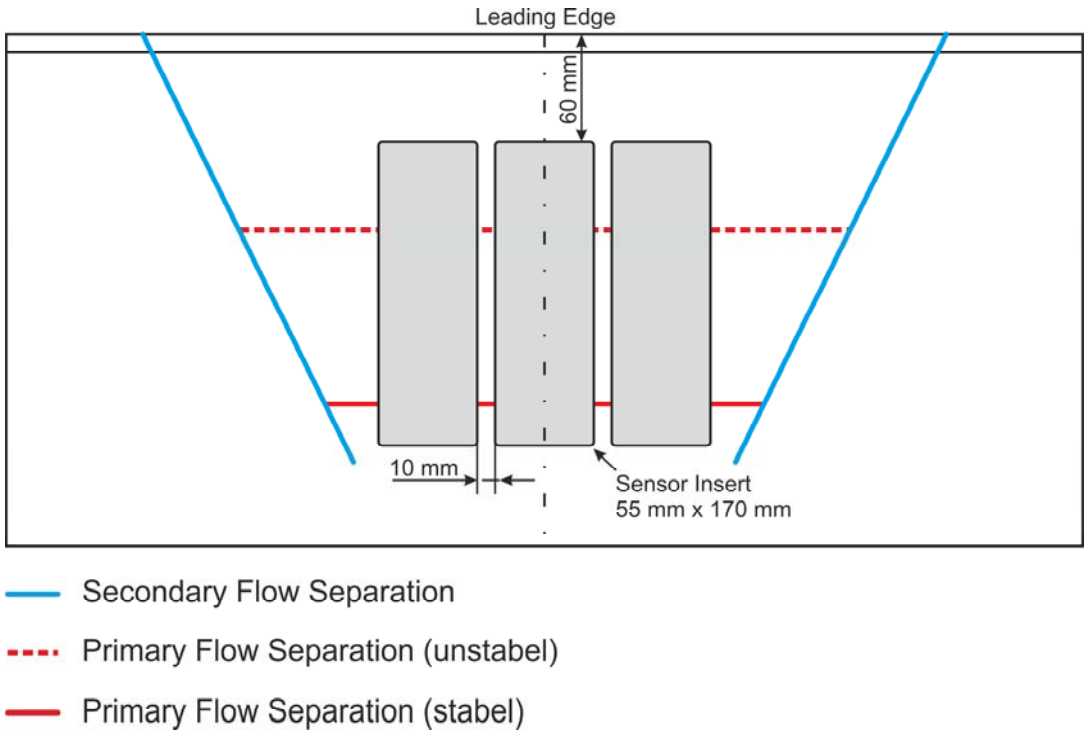

Figure 5: Sketch of the flap for the sensor tests with the results of the tuft visualisation for α = 19° and u_∞ = 20 m/s

Downstream of this position all tufts indicate flow separation. Comparing the two images shows that the separation onset moves to the leading edge of the flap with increasing flap angle. A flow velocity of u = 20 m/s was chosen for the experiments. This is a good compromise between high measurement values and the shift of the separation onset with the flap angle.

Sensor Tests

For the sensor test a new flap with three inserts was manufactured. As can be seen in Figure 5 the inserts have been positioned according to the results of the tuft visualisation. The inserts were positioned outside of the secondary flow separation. During the measurements the separation onset moves from the lower end of the inserts to the top for flap angles between α = 18° and α = 21°.

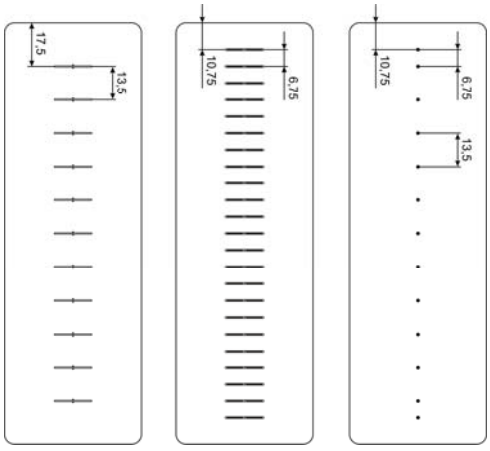

Figure 6: Sensor inserts

The inserts were equipped with different sensors and their positions were swapped during the sensor study to eliminate any influence of the spanwise position. One insert was equipped with a row of classic static pressure taps. The second insert was equipped with surface mounted hot wires. For reference measurements multiple surface wires have been applied to the third insert. Figure 6 shows a sketch of the three sensor inserts together with the sensor positions.

Sensors

For reference measurements 11 surface wires were employed. A detailed image of the sensor design is given in Figure 7, together with the universal calibration function. The sensor design is similar to a common surface fence. Two static pressure taps are placed on each side of a small obstacle which is placed in the viscous sublayer of the boundary layer. The measured pressure difference between the two static pressure taps is proportional to the wall shear stress. Additionally it is possible to determine the flow direction based on the sign of the pressure difference. If the diameter of the surface wire is the same as it is for the pressure taps a universal calibration function for the wall shear stress can be found. The calibration function shows a double logarithmic correlation between the non-dimensional wall shear stress

$$\tau_0^+ = \frac{\tau_w \cdot d^2}{4\rho\nu^2}$$

and the non-dimensional pressure difference

$$\Delta p_0^+ = \frac{\Delta p \cdot d^2}{4\rho\nu^2}$$

With the surface wire it was possible to perform an in situ calibration for the surface mounted hot wires as well. The calibration was conducted for a flap angle of α = 0° and different flow velocities between u = 3 m/s and u = 26 m/s. The design of the surface mounted hot wires is illustrated in Figure 8. A 5 µm wire is mounted over a small cavity. The cavity insulates both ends of the wire against each other and enables a flow around the wire. The cavities are manufactured by an etching process out of an printed circuit board (PCB). Afterwards the hot wires were welded over these cavities. The surface mounted hot wires are driven in constant temperature mode (CTA). Before analyzing the hot wire bridge signals a temperature compensation was applied to the signals to account for temperature fluctuations during the experiments.

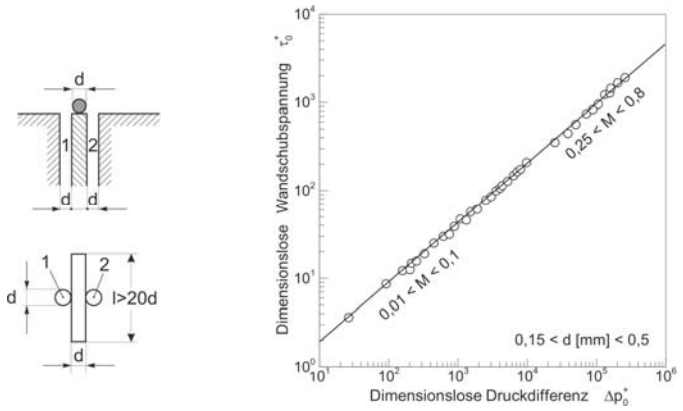

Figure 7: Surface wire

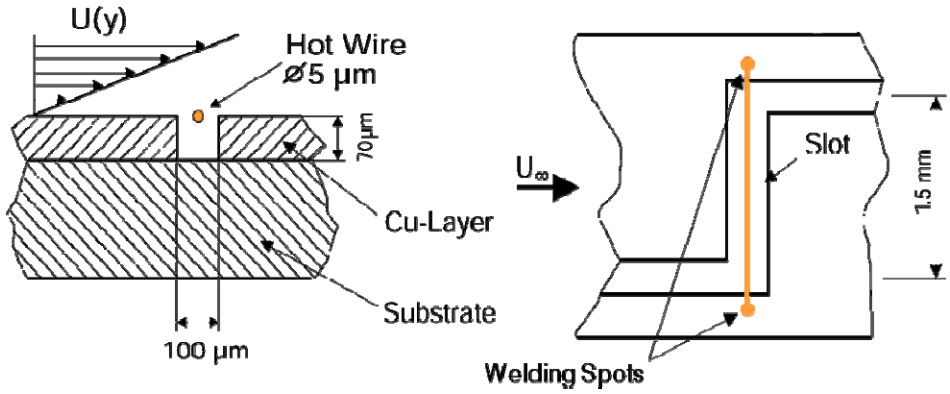

Figure 8. Surface mounted hot wire

The third insert was equipped with standard static pressure taps. For the measurements the same differential pressure transducers as for the surface wire were used. The static pressure at the test section inlet was used as reference pressure for this measurements. In case of a flow deceleration over the flap due to increasing flap angles, positive pressure differences were measured

$$\Delta p = p - p_{\infty}$$

Results

Figure 9 shows a contour plot of the static pressure difference for flap angles from alpha = 0° to alpha = 27°. The results are plotted over the sensor position. The first sensor position is located 87.5mm downstream of the junction between the flat plate and the flap, the last at 212.5mm. The sensors covered therefore 125 mm of the flap. For alpha = 0° a linear pressure distribution was measured with a negative pressure difference of Delta_p ≈ -15 Pa. The slight decrease is caused by a flow acceleration due to the growing boundary layers on the wind tunnel walls. Increasing the flap angle results in a continuous increase of Delta_p in the rear part of the flap. The maximum pressure difference on the flap is found at an angle of about alpha = 18°. Increasing the flap angle beyond this value results in a rapid pressure decrease on the flap. This indicates a flow separation on the flap. The lift coefficient c_A of the flap indicates this as well. Figure 11 shows the c_A distribution for the investigated flap angles. Up to alpha = 15.5° there is an linear increase for the c_A values. The plateau between alpha = 16° and alpha = 19,5° indicates a beginning flow

separation on the flap. Beyond alpha = 20° a rapid decrease of c_A shows that the flow is no longer attached to the flap. This results confirm the findings of the preliminary tuft visualization experiments. The static pressure distribution is well suited to detect a flow separation, but it is very difficult to detect the separation onset. Figure 12 shows the pressure distributions for selected flap angles.

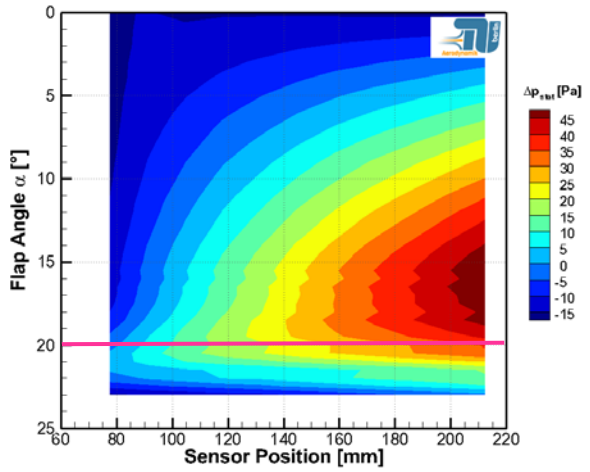

Figure 9: Static pressure difference for u_∞ = 20 m/

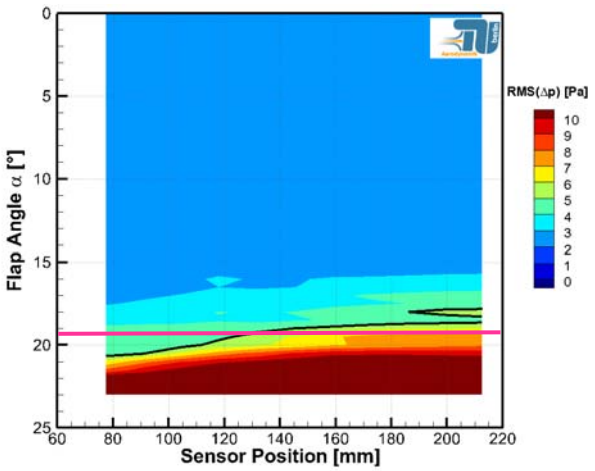

Figure 10: RMS(p) for u_∞ = 20 m/s

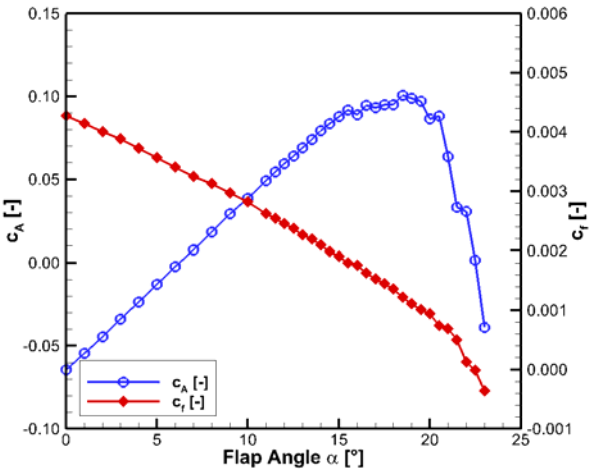

Figure 11: Lift and shear stress coefficient for u_∞ = 20 m/s

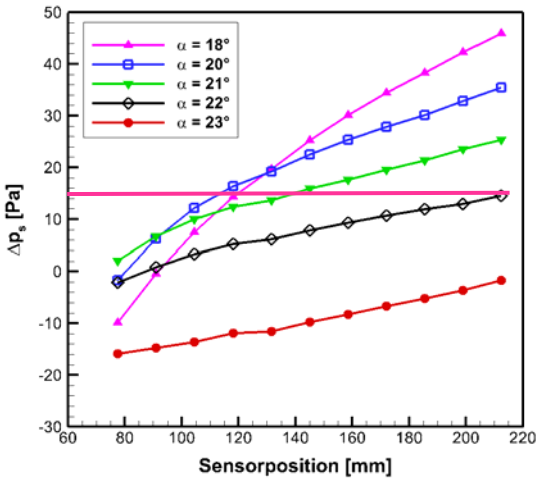

Figure 12: Pressure distribution for different flap angles

An obvious pressure plateau, which indicates a flow separation, can't be found for a > 18°. A Kink in the pressure distribution for alpha = 20° indicates that the flow is only partly separated. The flow is still attached to the flap up to a sensor position of 104.5mm. A better suited criterion to detect separation onset is the RMS value of the pressure fluctuations. Figure 10 shows the RMS values for the pressure measurements. In case of separation a increasing RMS values can be detected. For this reason it is possible to define a threshold value for the separation onset.

Another parameter to detect flow separation is the reversal of the flow direction in case of separation. The surface wire can detect this flow reversal. Figure 13 presents the results for the surface wire measurements. As can be expected the wall shear stress decreases with increasing flap angle. A partly flow separation for alpha = 20° cannot be detected in the results. The wall shear stress values are still positive. A flow reversal can firstly be detected for flap angles greater than alpha = 22°. The integrated wall shear stress coefficient c_f is shown in Figure 11 and shows a continuous decrease of the wall shear stress with increasing flap angles. The kink at alpha = 22° indicates the upcoming flow reversal. A similar results is obtained for the RMS values of the wall shear stress in Figure 14. A distinct increase of the fluctuations can only be detected for alpha = 22°. Compared with the pressure measurements and the tuft visualization the separation onset cannot be detected with the surface wires.

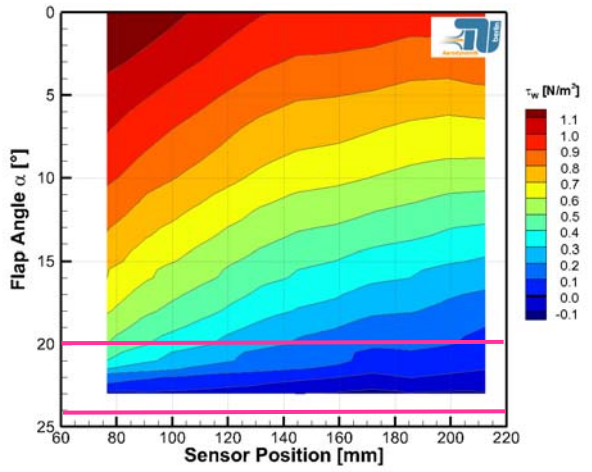

Figure 13: Surface wire results for u = 20 m/s

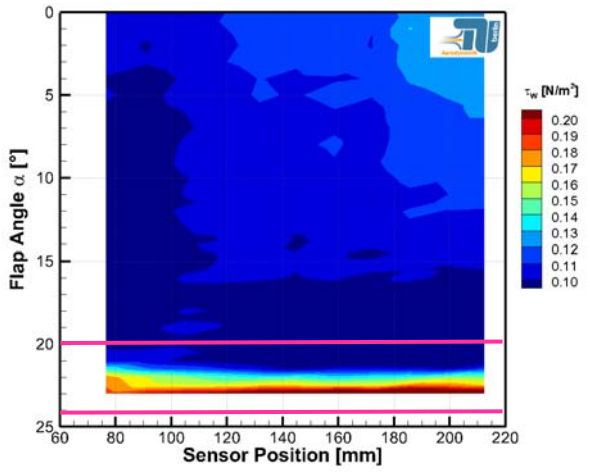

Figure 14: RMS(tau_w) for u = 20 m/s

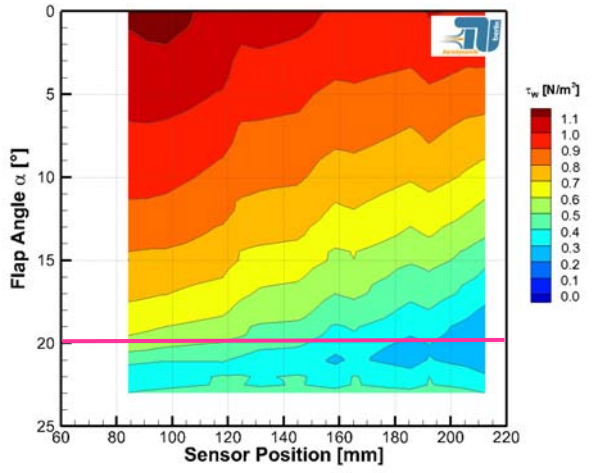

Figure 15: Surface hot wire results for u = 20 m/s

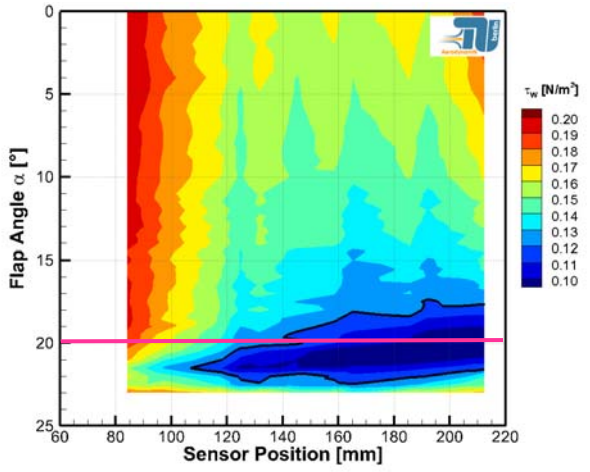

Figure 16: RMS(tau_w) for u = 20 m/s

The calibrated surface hotwires reveal similar results for the wall shear stress magnitude as can be seen in Figure 15. For small flap angles with an attached flow comparable shear stress values have been measured. But with increasing flap angles some differences can be observed between the two measurements, because the surface hotwire did not account for the flow direction. Therefore the absolute values for the wall shear stress begin to raise for flap angles greater than a = 22°. A flow separation can only be detected when the wall shear stress magnitude is less than a certain threshold value. A better criteria for separation control is the RMS value of the wall shear stress fluctuation. As can be seen in Figure 16, minimum RMS values occur in case of flow separation. The results are comparable to the pressure fluctuation measurements, but here the same phenomena is observed as for the wall shear stress magnitude. For alpha > 22° increasing values can be observed for the RMS values.

A flow separation can be detected normalising the pressure fluctuations with the wall shear stress magnitude. Figure 17 and Figure 18 show the results for the surface wire and the surface hot wire. The RMS values of the pressure measurements have been normalized with the wall shear stress values measured by the two sensor concepts. Both figures show very high values in case of a flow separation. A threshold value can be defined for both figures. In case of the surface wire this threshold is approximately RMS(p')/tau$_w$ = 20. For the surface hot wire a slightly lower value of RMS(p')/tau$_w$ = 15 is used. In both cases a separation onset at a sensor position close to 120mm can be detected, which is in good agreement with the tuft visualisation results. The combination of both measurement techniques reveals the best results detecting a flow separation. The large differences between an attaches flow and a separation makes this criteria relative robust against measurement disturbances.

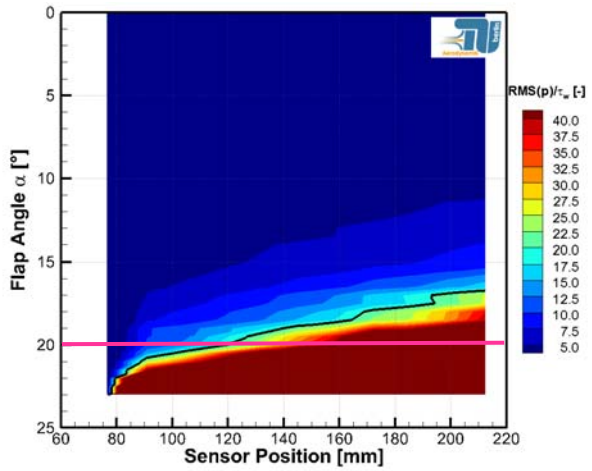

Figure 17: Surface wire results for RMS(p)/tau$_w$

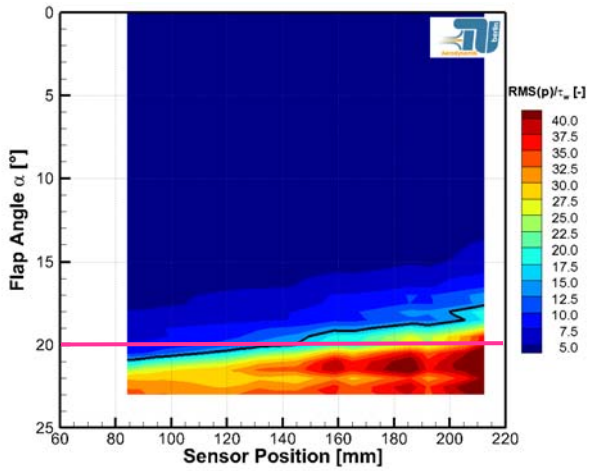

Figure 18: Surface hot wire results for RMS(p')/tau

The experiments show that a combination of the static pressure taps with the wall shear stress measurements provides the best results to determine a separating boundary layer. The quotient of the pressure fluctuations RMS(p') and the wall shear stress magnitude tau_w reaches values of $RMS(p')/tau_w > 20$ in case of flow separation. The large differences of the values between an attached flow field and a separation makes this criteria additionally insensitive against measurement errors and disturbances.

During the second period the focus was on the analysis of the wind tunnel test campaign performed at the end of the first project period. The task was to find a statistical parameter that describes the flow state and can be calculated directly out of the sensor data. Depending on the sensor type this parameter varies concerning the measured quantity and the spatial and temporal resolution of the sensor. Of special interest have been the sensors than can detect a flow reversal, because a flow reversal is a direct indicator for a flow separation.

For the evaluation of a suitable sensor concept the applicability to real aircraft wings was also taken into account, which makes the EADS hot-film sensors to the preferred concept. The EADS hot-film sensors are very flexible and can therefore be easily attached to the wing surface without affecting the structure of the wing. The pressure based sensor concepts require in most cases the drilling of micro holes to the wing surface, which weakens the structural integrity of the wing surface. Additionally, this micro holes can be blocked for example by dust and small particles. This blockage causes a failure of the single sensor.

The EADS hot-film sensors are more robust than conventional surface hot-wire sensors and can operate at standard flight conditions. The arrangement of the EADS hot-film sensors in an array of multiple sensors enables a high spatial resolution of the flow field if necessary. At the same time the EADS hot-film sensors offer a high temporal resolution, typical for hot-film and hot-wire sensors.

Taken all this aspects into account makes the bi-directional EADS hot-film sensors the concept of choice. With the arrangement of two hot-film sensors side by side it is possible to detect a flow reversal close to the surface. The EADS hot-film sensors seems to match all requirements to detect a flow separation on the wing surface. After the preliminary test on a simple straight flap this concept is tested on a wing model. The curvature of the surface makes a calibration of surface mounted sensors difficult. The final test of the EADS's hot-film sensors on the wing model focus on the detection of the flow reversal without performing a calibration of the sensors. By simply adjusting all sensors to a uniform level prior to the tests it is possible to detect a flow reversal which is sufficient to detect a flow separation.

EADS hot-film sensors

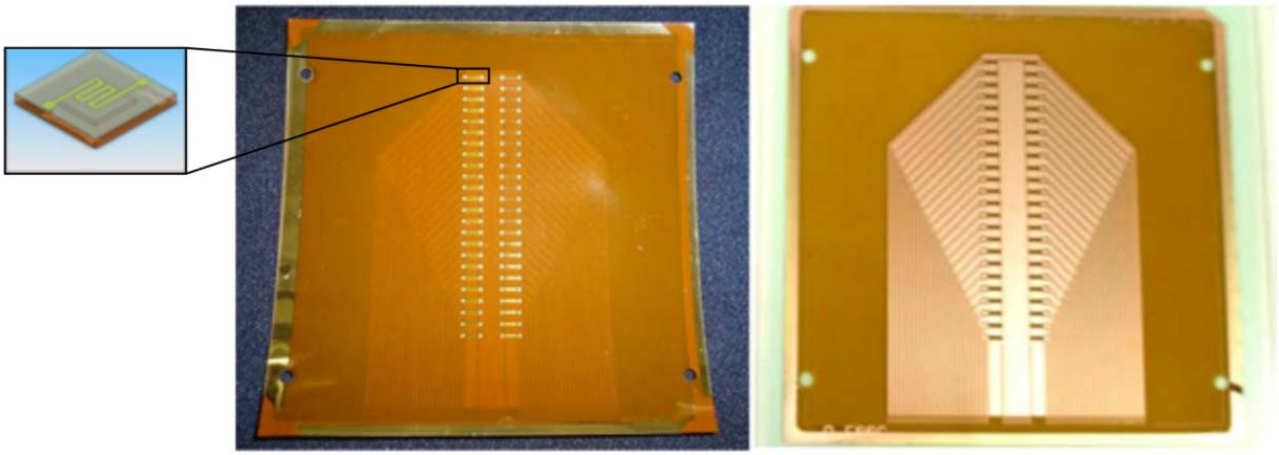

Figure 19: EADS hot-film sensor design

The EADS hot-film sensors are built on a flexible substrate, in order to allow mounting on curved surfaces. Contacting is provided by a structured copper layer located on the rear side of the sensor array and through connection to the sensing elements.

This sensor design is very favourable for measuring near wall velocity and wall shear stress, since it is thin enough to not influence the boundary layer. Furthermore, the sensing elements can be grouped easily into large arrays, hence allowing long measurment tracks. In the specific case of the EADS hot-film, the sensor array is composed of 48 sensing elements arranged in rows of 24 elements.

The microstructured hot-film sensors are also operated following the constant temperature anemometry principle (CTA) like the surface mounted hot-wires described before. They only differ in the design of the sensing element, which is a thin meandering shape gold film. In operation, the sensors are heated up to temperatures much higher than ambient. Typically, the sensor temperature is in the range of 100-300 °C. A detailed description can be found in.

According to the standard unidirectional design a bidirectional sensor layout was tested as well. Since the hot-film's sensing elements will have equal output signal, irrespective of the fluid flowing up- or downwards the sensor array, the sensor design has been modified in order to allow a differentiation between both cases. The sensing elements are arranged in pairs, the sensing elements of every pair being placed very closely behind one another. Thus, the upstream sensing element will heat up the fluid, reducing the cooling effect on the subsequent sensing element. Hence, its output voltage will be lower and it can be determined whether the fluid is flowing up- or downwards the array. Figure 20 shows an image of the bidirectional hot-film sensors.

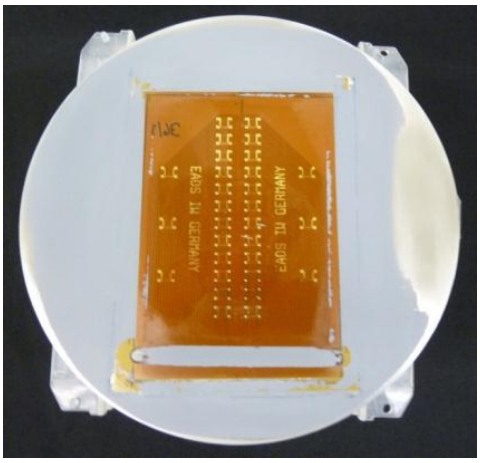

Figure 20: Bidirectional sensor layout

Results for the EADS hot-film sensors

According to the measurements with the classical sensor concepts presented in the last report, the EADS hot-film sensors have been tested to predict the separation onset on a simple flap test section. In conjunction with the surface wires a quasi-calibration was carried out for the hot-film sensors, which allows a comparison of the sensor signals with the prior shown measurement results. The measurements have also been carried out for an inflow velocity of u = 20 m/s and flap angles between α = 0° and α = 23°.

Figure 21 shows the measurement results for the unidirectional hot-film array. Figure 22 shows the sensor position on the vertical axis and the flap angle on the horizontal axis. Some sensors in the rear part of the array between a sensor position of a = 160 mm and a = 200 mm did not work in the correct manner and show a constant voltage value for all flap angles.

The mean voltage signal $\mu(u)$ is proportional to the wall shear stress τ_w presented in the plots in the last section. High values denote flow regions with high wall shear stress values. Whereas small sensor voltage values indicate flow regions with low wall shear stresses. Values beneath a certain threshold value therefore demark a flow separation.

As can be seen in Figure 21 the hot-film sensors show high voltage values for all sensor positions for flap angles up to α = 7°. A further increase of the flap angles results in a stronger deceleration of the flow and therefore to a reduction of the wall shear stress. Exceeding the critical flap angle of α = 18° results in a flow separation starting at the rear end of the plate (a = 200mm). This upcoming flow separation can be easily identified by the low sensor voltage values in Figure 21. In combination with the previous results a threshold values which indicates a flow separation can easily be defined for the present hot-film measurement. The pink line indicates the position and the flap angles where a flow separation can be detected on the flap. The results show that the flow separation shifts to the leading edge of the flap with increasing flap angles. This is the expected flow behaviour on the flap, and can be clearly be identified with the hot-film sensors used.

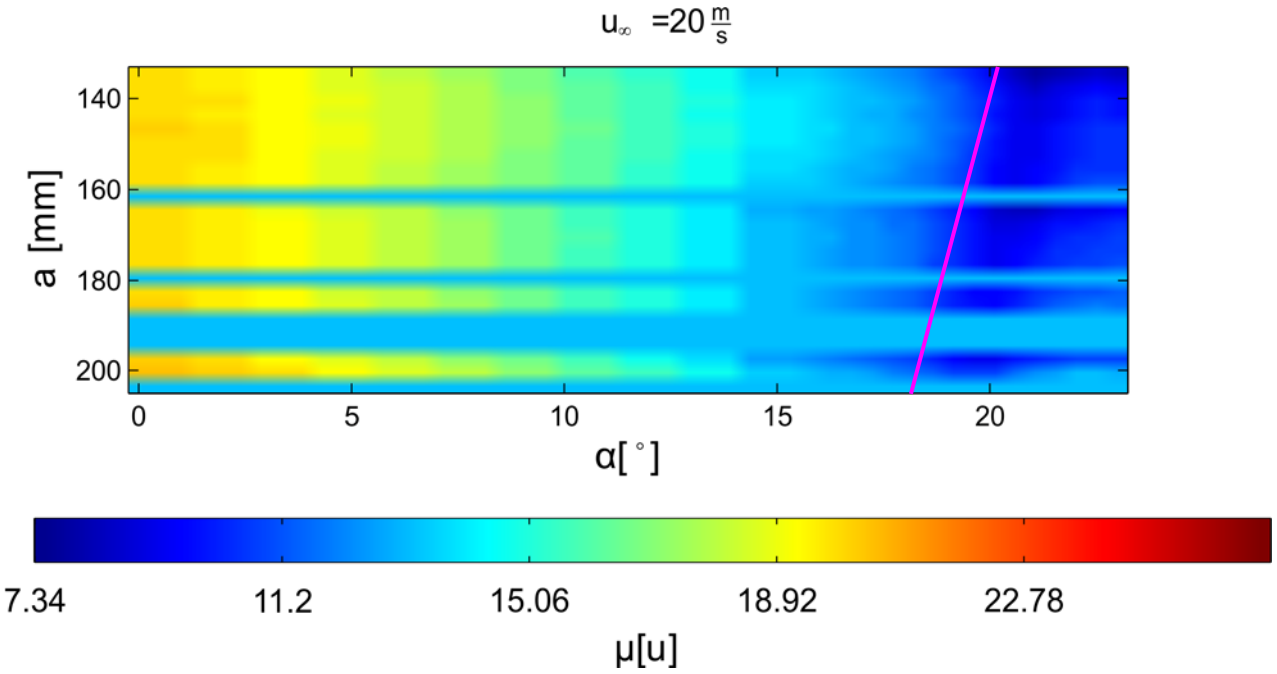

Figure 21: Mean voltage signals for the unidirectional hot-film sensors

The shift of the separation onset towards the leading edge of the flap with increasing flap angles a can also be observed in figure 22. The diagram shows the position of the minimum voltage value measured on the flap as a function of the flap angle. The result shows a linear shift of the flow separation with an increasing flap angle α. Figure 22 also shows that the minimum voltage value of the hot-film array is not suitable as a criteria to detect the separation onset, because the position of the minimum appears downstream of the separation onset. This becomes clear comparing the results of figure 22 with the results of the tuft visualisation. The visualisation results with the tufts show for a flap angle of α = 20° an upcoming flow separation at the position of a = 105mm. The minimum wall shear stress value measured with the hot-film array appears at a = 177mm. Nevertheless the single hot-film sensors can be used to detect the flow separation on the flap.

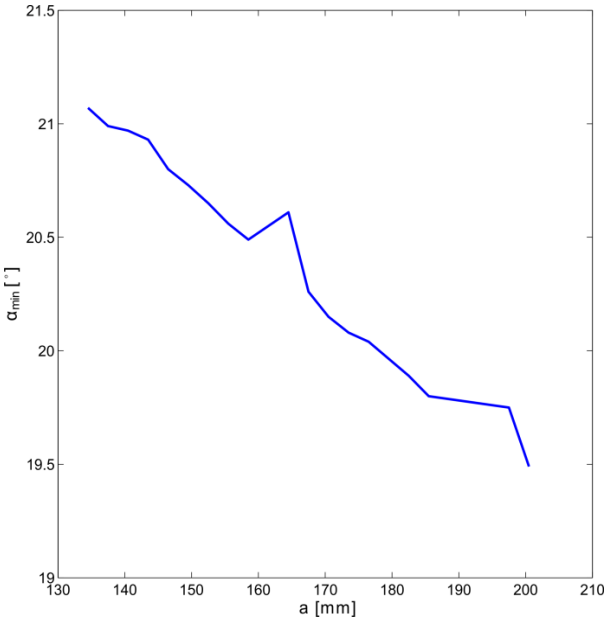

Figure 22: Position of the voltage-minimum measured with the unidirectional hot-films

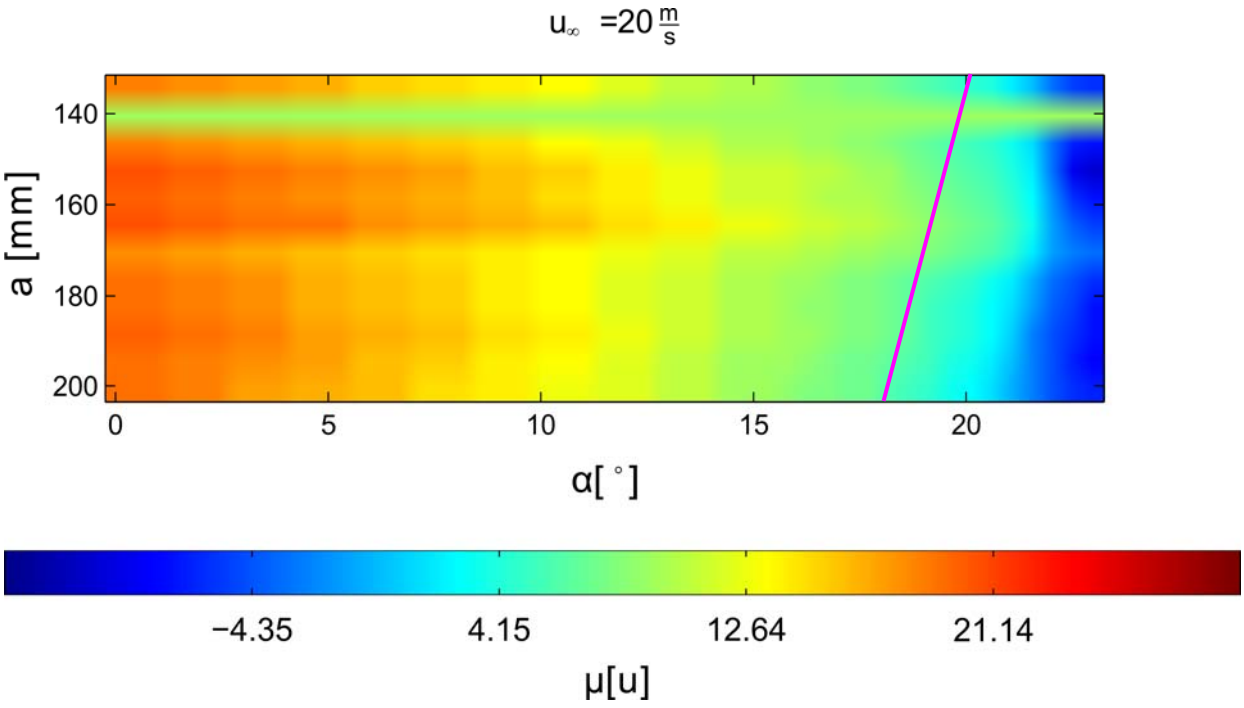

Figure 23: Mean voltage signals for the bidirectional hot-film sensors

A similar result can be obtained with the bidirectional hot-film array as can be seen in figure 23. The contour plot is similar to the results presented in figure 22. A comparison shows that the results in figure 23 cover a wider range of voltage values. Furthermore the bidirectional hot-films can detect a flow reversal which is indicated by the negative voltage values. Therefore the results for the bidirectional hot-film array show steeper gradients between the attached and the separated flow filed. This makes a separation detection

more easy and maore precise. The pink line demarks the position of separation onset extracted from the tuft visualisation. The results for the bidirectional hot-films show a steep gradient at this position. It can be seen that the separation onset starts when the hot-film voltage values are less than 7.5V, which is close to the offset of the single hot-film sensors. The flow reversal, which is linked to separation onset, causes the further reduction of the measured signals an seems to be a well suited criteria to detect the position of the separation onset on the flap.

The third period of FloSenSys dealt with the integration of the chosen fluidic sensor concept into a large scale wind tunnel model and the conduction and evaluation of the wind tunnel campaign.

The experiments were carried out at the GroWiKa facility of TU Berlin.

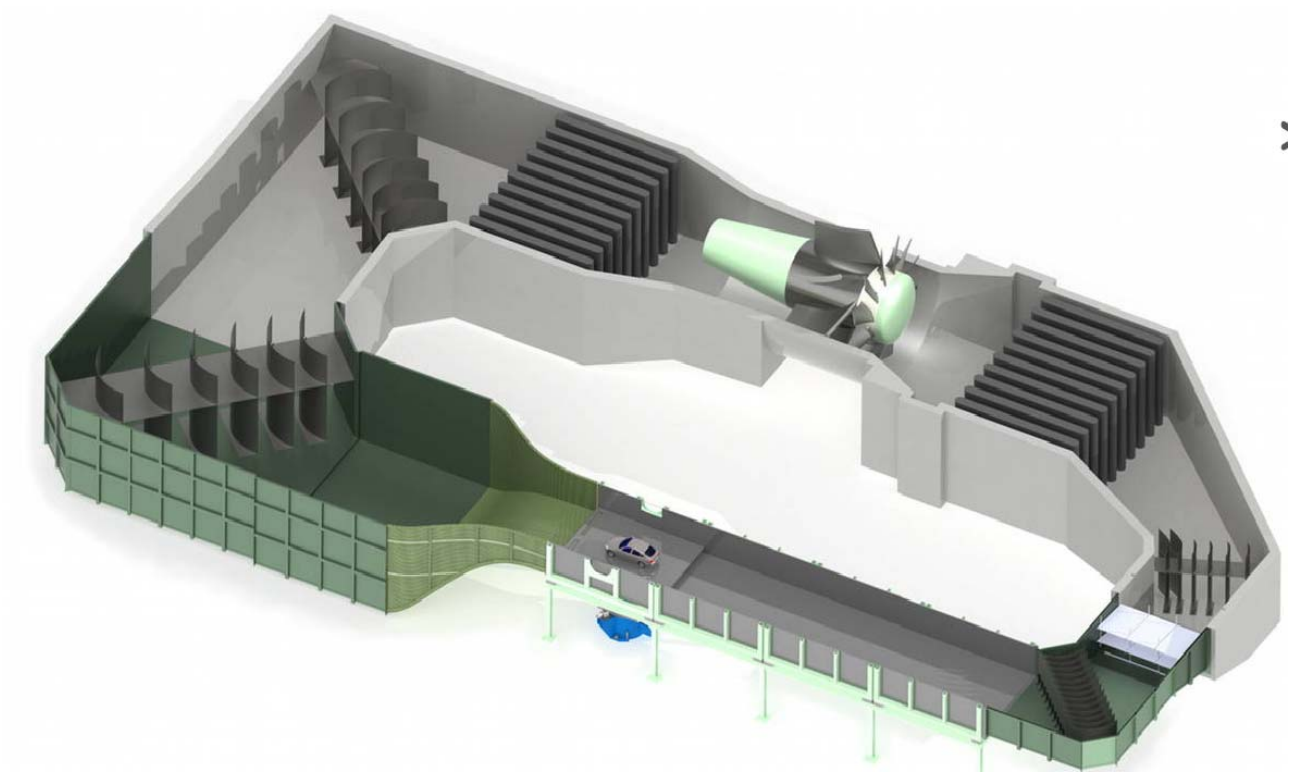

figure 24: 3D rendering of GroWiKa wind tunnel facility (source: http://fd.tu-berlin.de/en/facilities/wind-tunnels/growika/)

A sketch of this wind tunnel is shown in figure 24. It is a is a closed circuit wind tunnel with a 1400mm x 2000mm test section. The peak flow velocity is 50m/s.

The wind tunnel model employed for the final FloSenSys experiments is the complex outer wing section of a 3D wing. It is tapered and swept. A sketch of the model is shown in figure 25.

The span of the model measures 1040mm. Its reference chord length is 443mm. All experiments were conducted at a Reynolds number of Re = 1.05 * 10^6. Tripping was applied to ensure a turbulent state of the

boundary layer on the model and to minimize transition effects. Therefore two stripes of tape (40um high, 1mm wide) were attached at x/c = 0.1% and x/c = 0.5% on the pressure side of the model. At high incidence angles the stagnation point is located beyond that position on the pressure side and the tripping effects the suction side surface.

The model is mounted on a six-component strain gage balance located beneath the wind tunnel floor and forces and moments acting on the model were measured directly. The aerodynamic coefficients are calculated from those values. The model is equipped with 48 static pressure taps in two rows (at y/b = 42\% and y/b = 55\%) oriented in streamwise direction. The inner row comprises 30 stations on the suction and pressure surface, the outer row comprises 18 stations on the suction side surface only. In addition to those

quantitative methods of measurement oil and tuft flow visualization were employed to study the surface flow field. Rotating the balance around the y-axis allows for varying the angle of attack of the model.

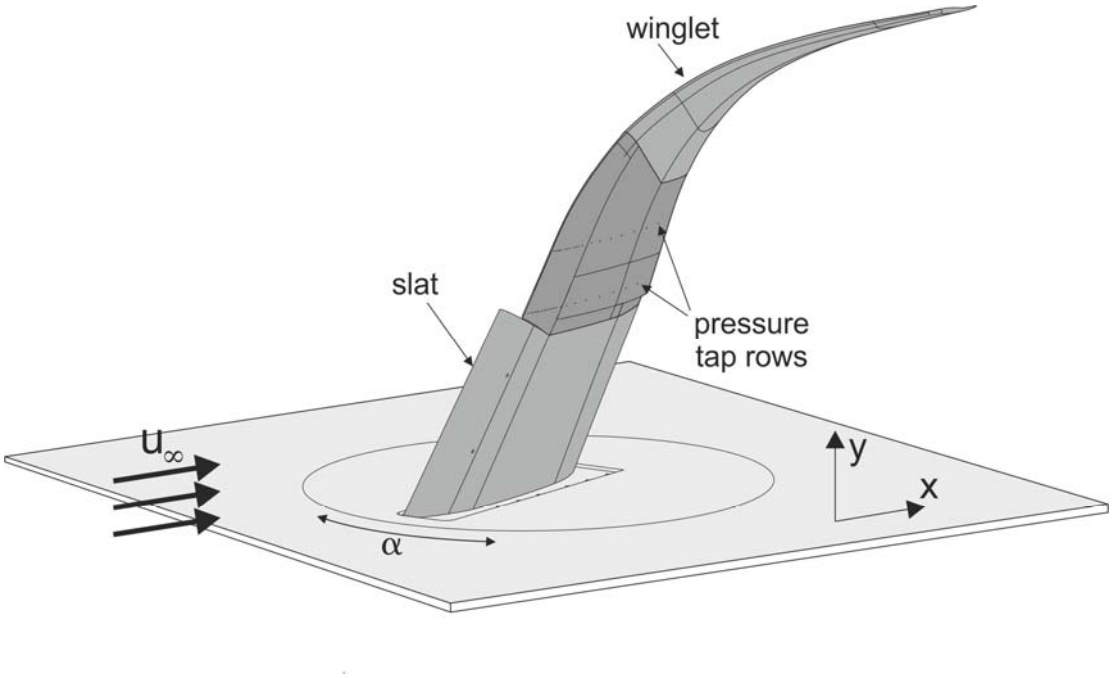

figure 195: sketch of wind tunnel model employed

The surface sensor system to be tested on this configuration is a thermal based sensor designed and manufactured by SFWA partner EADS-IW, the project partner for FloSenSys.

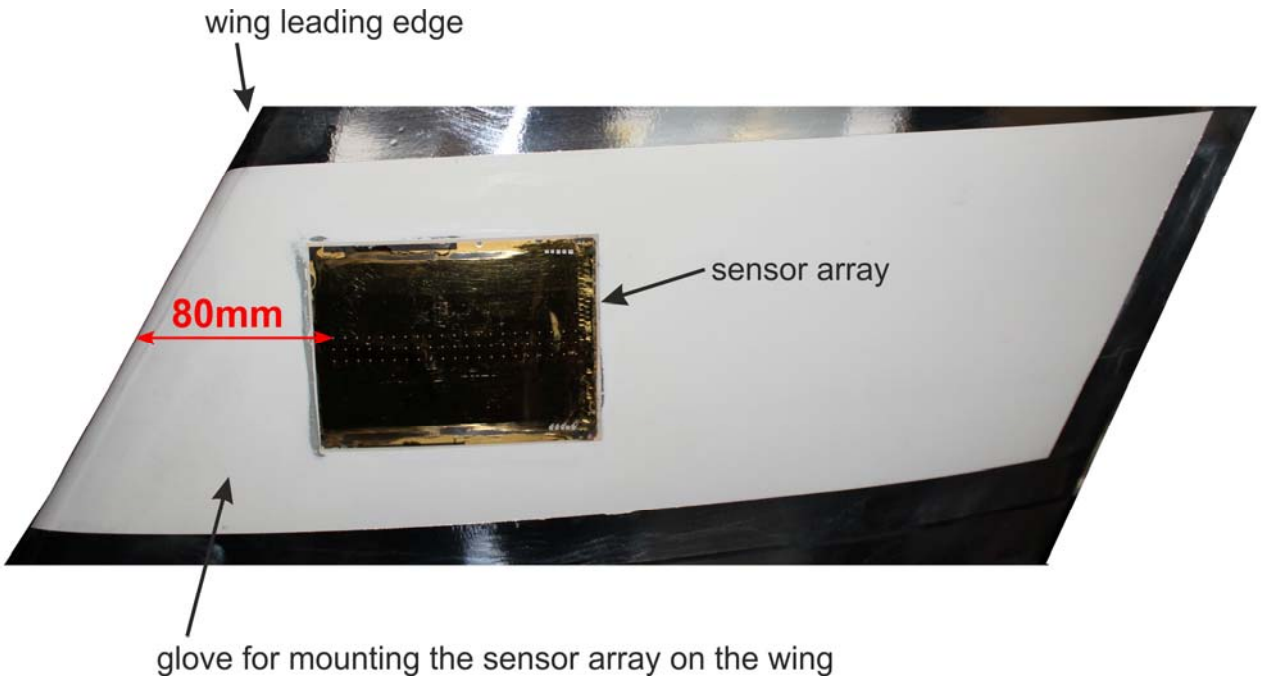

figure 26: surface sensor mounted on wing (source: EADS-IW)

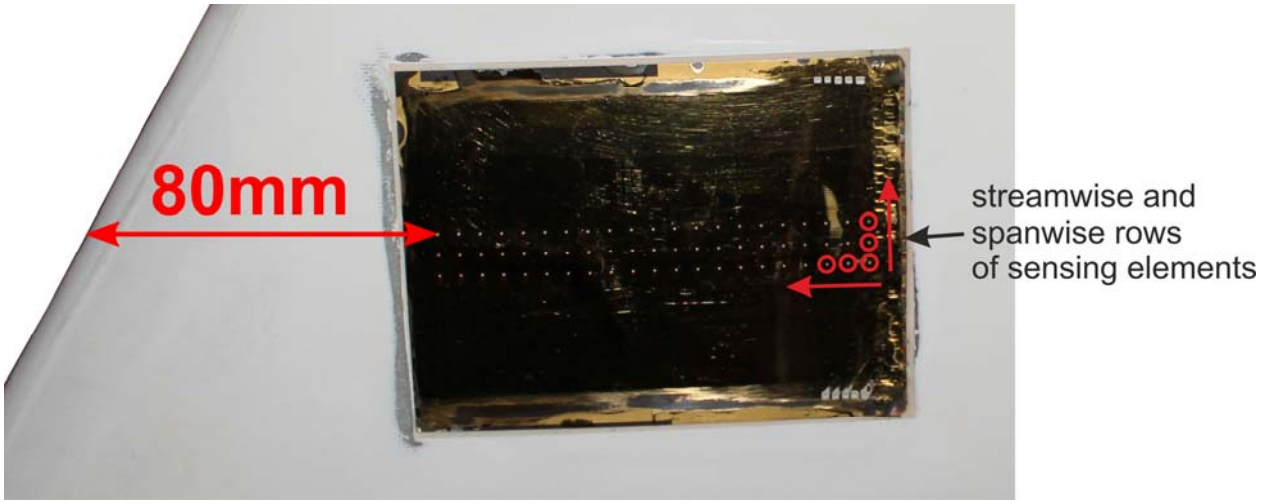

figure 27: detail view of sensor array on wing (source: EADS-IW)

Figures 26 and 27 show the layout of EADS-IW's sensor layout. The array is integrated at approximately 45% of spanwise position. It consists of 3 rows parallel to the oncoming flow several millimetres apart from each other. Each row comprises a total of 21 individual sensors.

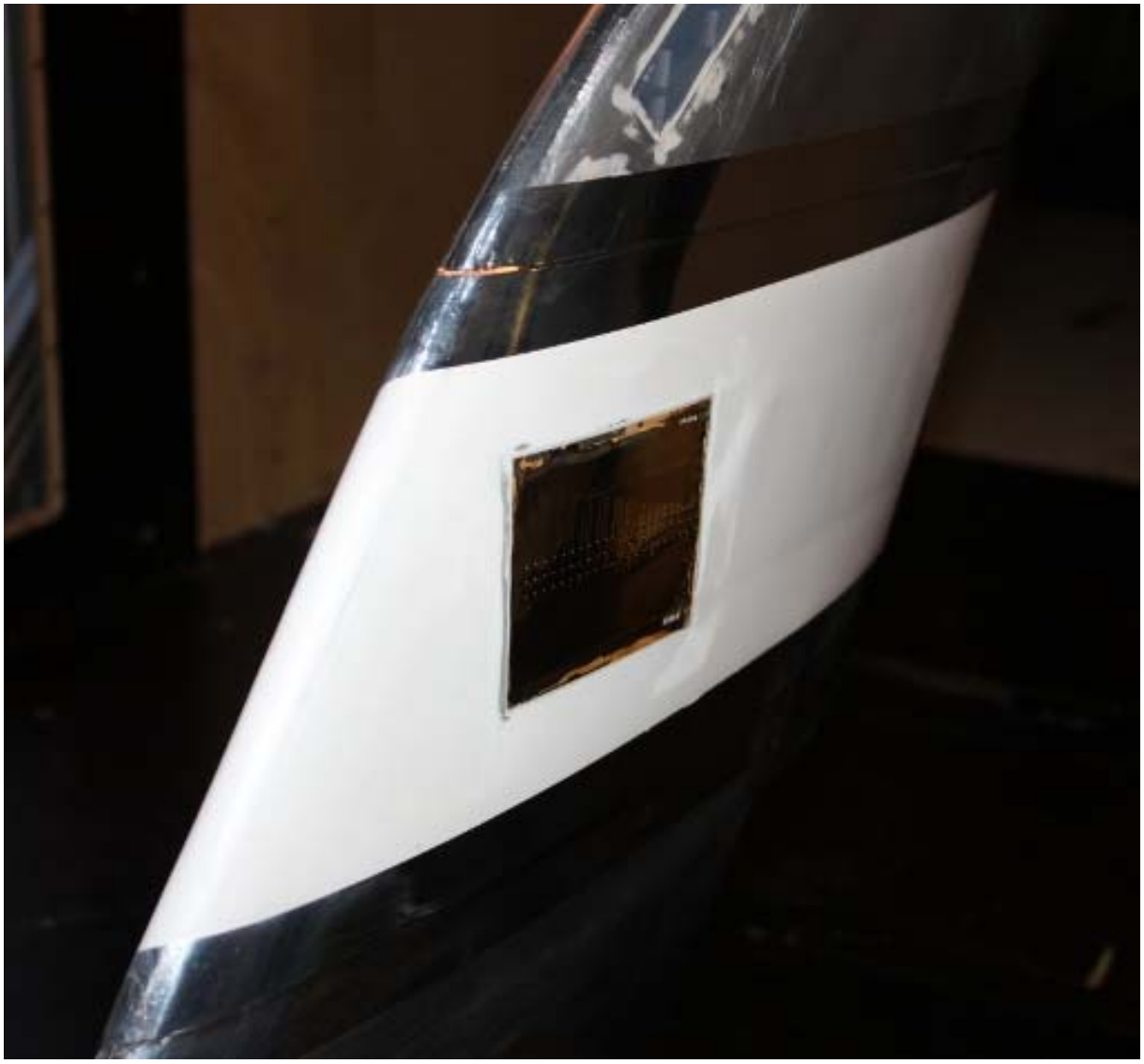

figure 28: model equipped with surface sensors

An image which shows the sensor array in relation to the leading edge is presented in figure 28.

The reference flow field is presented here and serves for later interpretation of the surface sensor results.

Tuft flow visualization was used to investigate direction and steadiness of the surface flow for the entire range of angles of attack tested. Observations for relevant angles of attack are presented in figure 29 through figure 31. For incidence angles much smaller than stall angle the surface flow is almost parallel to the direction of the oncoming flow. It shows no signs of unsteadiness with the exception of the region downstream of the slat edge and a small area near the trailing edge close to the wing tip. Flow unsteadiness increases significantly on the slatless section of the wing at an angle of attack close the stall angle (figure 30). The flow moves outward (towards the wing tip) in this region and although the measured lift force still increases occurrence of local separation is observable on the model's outboard section. Further increasing the angle of attack (figure 31) leads to a leading edge stall of the entire slatless section, with strong backflow

and highly unsteady flow direction. No separation is observed downstream of the slat up to 80% of chordwise position.

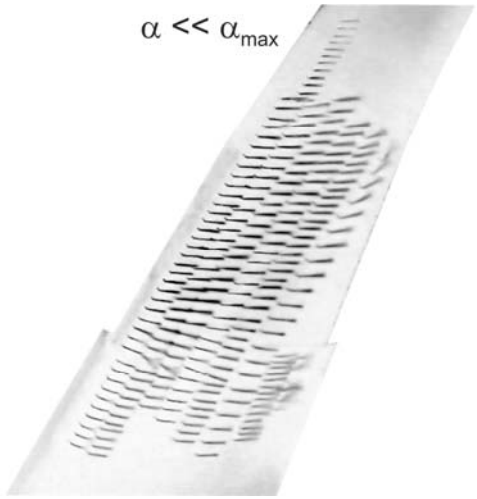

figure 29: tuft flow visualization for an angle before stall

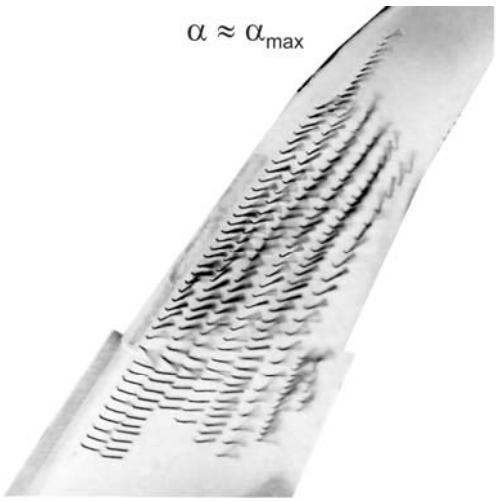

figure 30: tuft flow visualization at stall angle

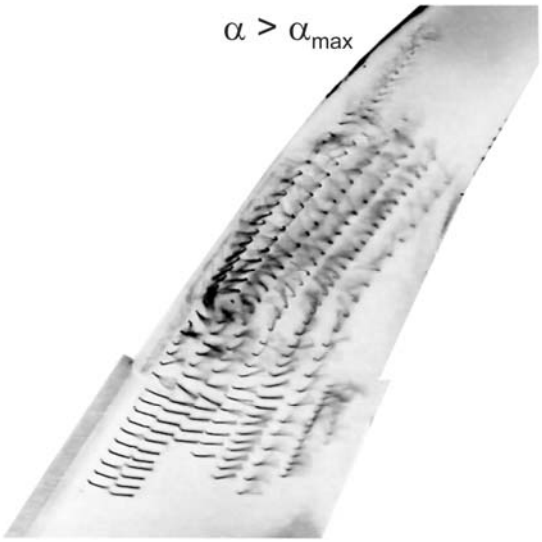

figure 31: : tuft flow visualization for an angle beyond stall

The characteristic topology of the separated flow is presented in figure 32. Oil flow visualization method was used to identify the features of the separated flow on the suction side surface of the wing. Two longitudinal vortices dominate the structures on the inboard half of the model. One strong longitudinal vortex is formed due to the interaction of the lifting surface and the wind tunnel wall, which increases in strength and diameter with increasing angle of attack. This feature would not be present on a full wing. The second longitudinal vortex forms at the slat edge (slat edge vortex). It causes the local streamlines to curve towards the wingtip. When the stall angle of attack is reached, the flow separates abruptly from the surface. The separation line is located at approximately 10% of x/c position with strong backflow trailing the separation. Next to the slat edge vortex a recirculation region (rotating in counterclockwise sense) is formed reaching up to x/c = 2% of chord position.

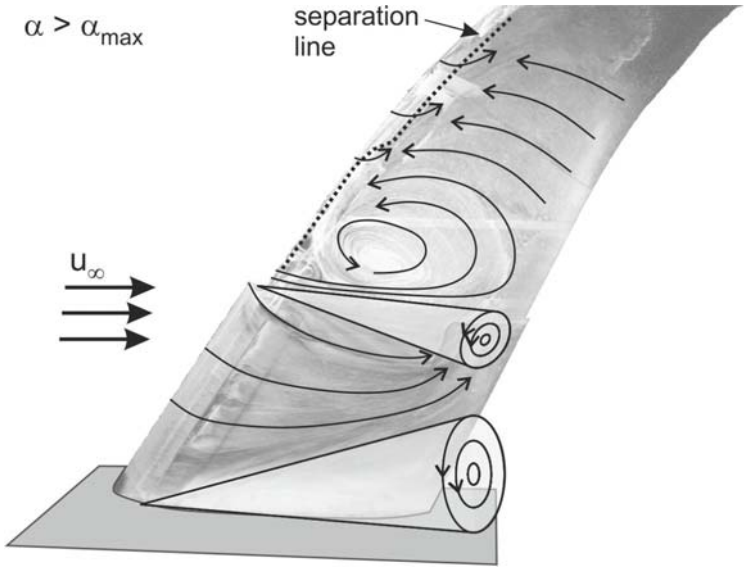

figure 32: oil flow visualization and characteristic topology

Results from force measurements for the uncontrolled flow are presented in figure 33. This is the reference data to which the controlled cases are compared to. The maximum angle of attack is defined as the angle for which the highest lift coefficient is observed. Further increasing the incidence angle results in a sudden increase in drag and a drop in aerodynamic efficiency.

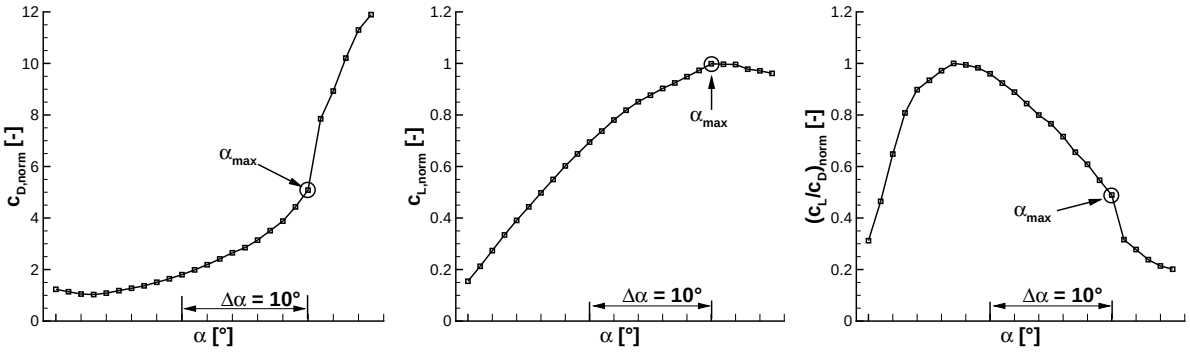

figure 33: drag, lift and aerodynamic efficiency from force measurements

EADS-IW's surface sensor measures convective heat transfer and outputs a voltage signal from which the state of the flow can be inferred. Figure 34 shows preliminary results for one individual active segment of the sensor array for increasing angles of attack.

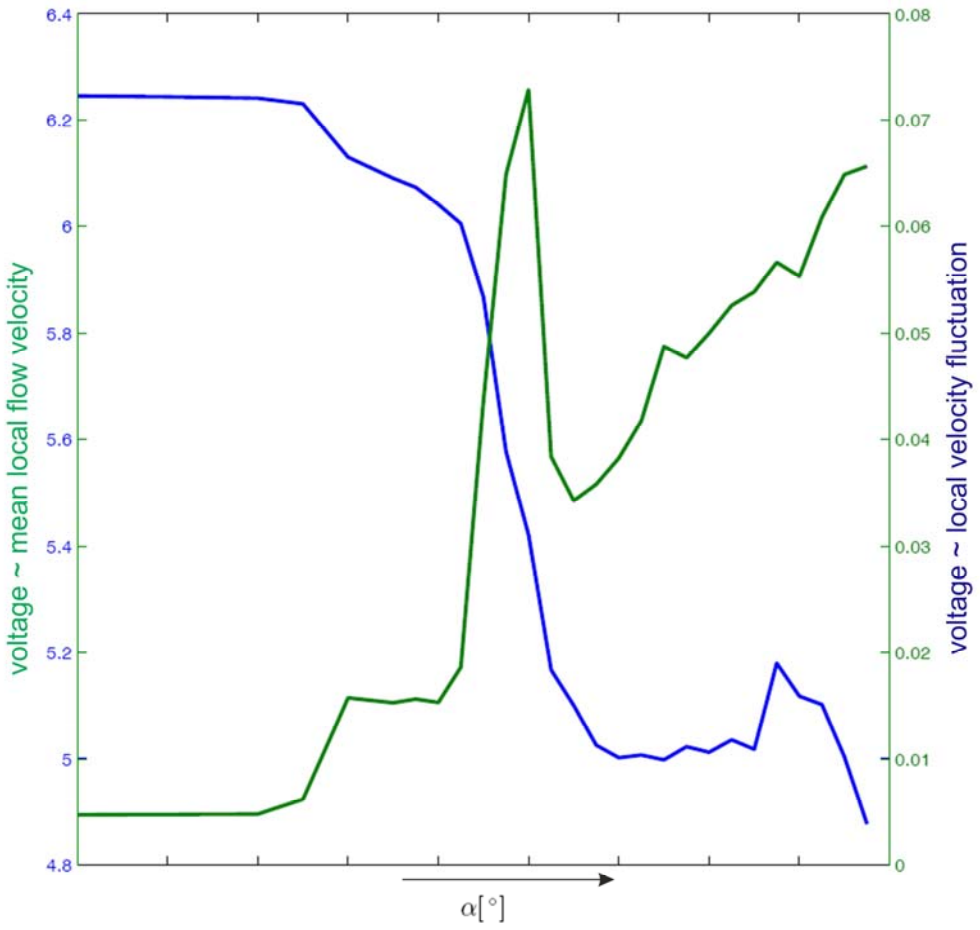

figure34: preliminary results from EADS-IW's surface sensor (source: EADS-IW)

When separation occurs the curve associated with the mean flow velocity drops by approximately 20% and settles at a lower level for all consecutive angles. In contrast to that the curve associated with the velocity fluctuation peaks at the onset of stall. The sensor therefore allows to identify the state of the flow on the wing. More extensive analysis of the wind tunnel results obtained with this surface sensor will be reported by EADS-IW within the frame of consortium reporting.

Potential impact and exploitation of results

The experiments showed the feasibility of implementing an AFC sensor system for realistic flow conditions. The work conducted - in cooperation with SFWA partner EADS-IW - lead to deeper understanding of how such a system can be best designed for being applicable on a civil airliner and increased the available data basis for flow sensors in the light of flight application.

For this project the assumed business case was e.g. the replacement of a double slotted flap by a smaller single slotted flap. The AFC system for such an approach was researched and developed in the SFWA CfP projects AFCIN, FloCoSys, and DT-FA-AFC. Within this frame FlowSenSys can contribute to providing a sensing system to realize a closed-loop flow control architecture to achieve a more effective and efficient flow control authority. Besides a possible reduction of system weight, tipple down benefits are the reduction of the flap size (therefore freeing up additional space in the main wing element) and the reduction of maintenance costs (by reducing the system complexity compared to a double slotted flap).

The results of this project can serve as input for upcoming and ongoing projects. For further large scale testing or flight experiments an flow sensing system stands ready to be integrated.

Relevant contact details

Prof. Dr.-Ing. Wolfgang Nitsche
Fachgebiet Aerodynamik, Sekr. F2, Technische Universität Berlin
Marchstrasse 12-14
10587 B e r l i n
www.aero.tu-berlin.de